Mapping Mouse Gamete Interaction Forces Reveal Several Oocyte Membrane Regions with Different Mechanical and Adhesive Properties†

Antoine Jégou,‡ Frédéric Pincet,‡ Eric Perez,‡ Jean Philippe Wolf,§ Ahmed Ziyyat,§ and Christine Gourier*,‡

Laboratoire de Physique Statistique de l'Ecole Normale Supérieure de Paris, UMR 8550 associée au CNRS et aux Universités Paris 6 et Paris 7, 24 rue Lhomond, 75005 Paris, France, and Laboratoire Protéines membranaires et interaction gamétique, UFR SMBH, Université Paris 13, Bobigny, France

Received July 25, 2007. In Final Form: September 12, 2007

This study focuses on the interaction involved in the adhesion of mouse gametes and on the mechanical properties of the oocyte membrane. The oocyte has an asymmetrical shape, and its membrane is composed of two distinct areas. One is rich in microvilli, and the other is smoother and without microvilli. With a biomembrane force probe (BFP) adapted to cell−cell measurements, we have quantified the separation forces between a spermatozoon and an oocyte. Microvillar and amicrovillar areas of the oocyte surface have been systematically probed and compared. In addition to a substantial difference in the elastic stiffness of these two regions, the experiments have revealed the presence of two types of membrane domains with different mechanical and adhesive properties, both distributed over the entire oocyte surface (i.e., in both microvillar and amicrovillar regions). If gamete contact occurs in the first type of domain, then the oocyte membrane deforms only elastically under traction. The pull-off forces in these domains are higher in the amicrovillar region. For a spermatozoon contact with the other type of domain, there can be a transition from the elastic to viscoelastic regime, and then tethers are extruded from the oocyte membrane.

Introduction

Mammalian fertilization consists of a series of events leading to the creation of a new being through the merging of a spermatozoon and an oocyte. The oocyte plasma membrane has two distinct regions: the first one is covered with microvilli, and the second one is smaller, without microvilli. In the latter region, fusion rarely, if ever, occurs.[1−4] Why fusion preferentially takes place in the microvillar area is still unclear. One possible explanation is that binding sites on oocytes for spermatozoon ligands are located in specific domains on the egg surface.[5,6]

According to Runge et al.,[7] microvilli could act as a platform to concentrate adhesion/fusion proteins and/or provide a membrane protrusion with a low radius of curvature favorable for membrane fusion.[8,9] A direct measurement of the interaction forces involved when an oocyte and a spermatozoon adhere in both areas may validate such a hypothesis. Another explanation of the differences between microvillar and amicrovillar areas may come from the mechanical properties of the oocyte membrane. These have not yet been characterized and remain to be explored. To detect and quantify local changes in membrane deformability and adhesion behavior on a micrometer length scale, a nanoforce technique is required.

A number of advanced techniques have been developed to investigate cell−substrate and cell−cell interactions. The parallel plate flow chamber,[10,11] the atomic force microscopy technique (AFM),[12,13] the surface force apparatus (SFA),[14] and the biomembrane force probe (BFP)[15] were used to characterize single ligand receptor systems through their kinetic parameters[10,11] and energy landscape.[16−18] Dual micropipette techniques were used to test the adhesion energies of biological model systems such as giant vesicles[19−23] or rupture forces involved between two cells overexpressing adhesion proteins.[24−26] AFM[27−32] and

† Part of the Molecular and Surface Forces special issue.

* Corresponding author. E-mail: gourier@lps.ens.fr.

‡ UMR 8550 associée au CNRS et aux Universités Paris 6 et Paris 7.

§ Université Paris 13.

(1) Yanagimachi, R., Mammalian fertilization. In *The Physiology of Reproduction*; Knobil, E., Neil, J., Eds.; Raven Press Ltd.: New York, 1994.

(2) Johnson, M.; Eager, D.; Muggleton-Harris, A.; Grave, H. *Nature* **1975**, *257*, 321−322.

(3) Nicosia, S.; Wolf, D.; Inoue, M. *Dev. Biol.* **1977**, *57*, 56−74.

(4) Ebenspenger, E.; Barros, C. *Gamete Res.* **1984**, *9*, 384−397.

(5) Rubinstein, E.; Ziyyat, A.; Wolf, J. P.; Le Naour, F.; Boucheix, C.; *Semin. Cell Dev. Biol.* **2006**, *17*, 254−263.

(6) Ziyyat, A.; Rubinstein, E.; Monier-Gavelle, F.; Barraud, V.; Kulski, O.; Prenant, M.; Boucheix, C.; Bomsel, M.; Wolf, J. P. *J. Cell Sci.* **2006**, *119*, 416−424.

(7) Runge, K. E.; Evans, J. E.; He, Z. Y.; Gupta, S.; McDonald, K. L.; Stahlberg, H.; Primakoff, P.; Myles, D. G. *Dev. Biol.* **2007**, *304*, 317−325.

(8) Monroy, A. *Eur. J. Biochem.* **1985**, *152*, 51−56.

(9) Wilson, N. F.; Snell, W. J. *Trends Cell. Biol.* **1998**, *8*, 93−96.

(10) Perret, E.; Benoliel, A. M.; Nassoy, P.; Pierres, A.; Delmas, V.; Thiery, J. P.; Bongrand, P.; Feracci, H. *EMBO J.* **2002**, *21*, 2537−2546.

(11) Pierres, A.; Touchard, D.; Benoliel, A. M.; Bongrand, P. *Biophys. J.* **2002**, *82*, 3214−3223.

(12) Moy, V. T.; Florin, E. L.; Gaub, H. E. *Science* **1994**, *266*, 257−259.

(13) Florin, E. L.; Moy, V. T.; Gaub, H. E. *Science* **1994**, *264*, 415−417.

(14) Jeppesen, C.; Wong, J. Y.; Kuhl, T. L.; Israelachvili, J. N.; Mullah, N.; Zalipsky, S.; Marques, C. M. *Science* **2001**, *293*, 465−468.

(15) Evans, E.; Ritchie, K.; Merkel, R. *Biophys. J.* **1995**, *68*, 2580−2587.

(16) Evans, E.; Williams, P. M. Dynamic Force Spectroscopy. In *Physics of Bio-Molecules and Cells*; Julicher, F., Ormos, P., David, F., Flyvbjerg, H., Eds.; Springer-Verlag: Berlin, 2002; pp 145−204.

(17) Evans, E.; Leung, A.; Heinrich, V.; Zhu, C. *Proc. Natl. Acad. Sci.* **2004**, *101*, 11281−11286.

(18) Pincet, F.; Husson, J. *Biophys. J.* **2005**, *89*, 4374−81.

(19) Evans, E. *Colloids Surf.* **1990**, *43*, 327−347.

(20) Pincet, F.; Le Bouar, T.; Zhang, Y.; Esnault, J.; Mallet, J. M.; Perez, E.; Sinay, P. *Biophys. J.* **2001**, *80*, 1354−1358.

(21) Pierrat, S.; Brochard-Wyart, F.; Nassoy, P. *Biophys. J.* **2004**, *87*, 2855−2869.

(22) Gourier, C.; Pincet, F.; Perez, E.; Zhang, Y. M.; Zhu, Z. Y.; Mallet, J. M.; Sinay, P. *Angew. Chem., Int. Ed.* **2005**, *44*, 1683−1687.

(23) Gourier, C.; Pincet, F.; Perez, E.; Zhang, Y. M.; Mallet, J. M.; Sinay, P. *Glycoconjugate J.* **2004**, *21*, 165−174.

(24) Chu, Y. S.; Dufour, S.; Thiery, J. P.; Perez, E.; Pincet, F. *Phys. Rev. Lett.* **2005**, *94*, 028102.

(25) Martinez-Rico, C.; Pincet, F.; Perez, E.; Thiery, J. P.; Shimizu, K.; Takai, Y.; Dufour, S. *J. Biol. Chem.* **2005**, *280*, 4753−4760.

(26) Daoudi, M.; Lavergne, E.; Garin, A.; Tarantino, N.; Debre, P.; Pincet, F.; Combadiere, C.; Deterre, P. *J. Biol. Chem.* **2004**, *279*, 19649−19657.

10.1021/la702258x CCC: $40.75
Published on Web 11/21/2007

microplate techniques[33,34] were used to study the adhesive properties of single cells on substrates and cell−cell adhesion. The mechanical properties and microstructure of cells or giant vesicles were probed with optical tweezers,[35−37] with the micropipette aspiration technique,[38,39] and with the BFP.[40−42] Among these studies, very few involved direct cell−cell interactions.

In this study, we aim to investigate the interaction and mechanical properties of two primary cells, an oocyte and a spermatozoon, which in nature are destined to meet and adhere in order to fuse and produce a new being. Our first approach consisted in a qualitative observation of the adhesive and mechanical response of the two gamete membranes when, after a contact time of a few seconds to a few minutes, the spermatozoon and the oocyte were pulled apart with micropipettes. Observations were made by direct and fluorescence light microcopy and have revealed the presence of tethers between the two cells. Tether formation is not unheard of[32,35−38,40−43] and has been observed in various systems, but this is the first evidence that the interaction between two primary cells is capable of giving rise to tethers. To investigate in a more quantitative way the adhesion behavior and mechanical properties of the gamete membranes and their potential local variations, the BFP technique has been adapted for direct cell−cell measurement. This was made possible by the small size and suitable morphology of the spermatozoon head that allowed its fixation on the bead of the BFP transducer. The spermatozoon head can be seen as flat with dimensions of approximately $5 \times 3 \times 1\ \mu m^3$. The oocyte is around 80 μm in diameter. This difference in size leads to a small contact area (about 10 μm^2) between the two gametes and offers the opportunity to select the contact location on the oocyte membrane carefully. Moreover, by controlling the contact time, the cell−cell binding can be reduced to a single attachment point. We cannot know whether this single attachment point corresponds to single molecules or to single molecular complexes.

A strong difference in the membrane elastic stiffness has been established between microvillar and amicrovillar areas of the oocyte surface. Less intuitively, two types of domains providing locally different mechanical responses have been observed both in amicrovillar and microvillar areas. No tether could ever be formed in the first domains whereas a tether could be extruded when in the second ones. Tether extrusion was characterized by a viscoelastic regime during the separation of the cells. Similar membrane behavior has recently been reported by Evans and co-workers[41,42] on human neutrophils (PMN) with PSGL-1 receptors interacting with P-selectin-decorated beads. Like the microvillar region of the oocyte, PMN cells were rich in microvilli. Here, we show that tethers can also be extruded from amicrovillar surfaces. The distribution of these domains on the oocyte membrane and the forces involved in the oocyte−spermatozoon separation are also discussed.

Materials and Methods

Gamete Preparation. *Sperm Preparation.* Spermatozoa have been prepared as previously described.[6] B6CBA male mice (8−10 weeks old) were purchased from Charles River Laboratories. For sperm isolation, the two caudae epididymis and vas deferens were removed from an adult mouse. Sperm were gently expelled from the caudae epididymis into a 300 μL drop of ferticult medium (FertiPro, Belgium) with 3% bovine serum albumin (BSA, Sigma-Aldrich, Lyon, France) under mineral oil. Spermatozoa were incubated at 37 °C in 5% CO_2 for 90 min to induce capacitation and acrosome reaction, giving the spermatozoa the ability to fuse with the oocyte. A mouse spermatozoon is composed of an almost flat head and a 60-μm-long flagellum.

Oocyte Preparation. The oocytes have been prepared as previously described.[6] B6CBA female mice (6−8 weeks old) were purchased from Janvier Laboratories. They were superovulated by two sequential intraperitoneal injections of 5 IU PMSG (Folligon, Intervet, France) and, 48 h later, 5 IU hCG (Chorulon, Intervet, France). Fourteen hours after hCG injection, cumulus−oocyte complexes were collected by tearing the oviductal ampulla after the mice were sacrificed. Oocytes were separated from the cumulus by incubating the complexes in the presence of hyaluronidase (15 mg/mL) at 37 °C for 1 min. Finally, the zona pellucida surrounding the oocyte was removed by treatment for 30 s in pure acidic Tyrode's solution (Sigma-Aldrich, Lyon, France). Mature oocytes were selected on the basis of the clean aspect of the cytoplasm and the presence of the first polar body. Oocytes are stored for 3 h at 37 °C in 5% CO_2 for recovery.[44,45] In mice, oocytes are around 80 μm in diameter and are pear shaped with two distinct plasma membrane regions (Figure 1A). The first one is covered with microvilli of typically 300 nm height. The second one (∼30% of the total membrane surface) is overlying the meiotic spindle and lacks microvilli.[46] The texture difference between the two regions can easily be observed by electron microscopy (as reported by Runge et al. in ref 7, Figure 1A). With optical microscopy, the two regions are discriminated through the shape of the oocyte, with the amicrovillar region being the top of the pear (labeled by the star in Figure 1A).

Fluorescence Microscopy. Experiments were performed at room temperature on oocytes and spermatozoa prepared as mentioned above. The oocytes were incubated for 45 min at 37 °C in 5% CO_2 in ferticult medium containing an anti-CD9 rat antibody coupled with goat anti-rat Alexa Fluor 594 (gift from C. Boucheix, Villejuif, France) at 10 μg/mL. After gentle rinsing of the oocytes, a spermatozoon was manipulated with a micropipette and brought into contact with the microvillar region of a single oocyte for 5 min. Cells were then separated to a distance of around 20 μm. The observation was made on a Leica DM-IRB inverted microscope in epifluorescence under the excitation of an argon lamp. The fluorescence and direct light images were acquired by a Hamamatsu C5985 camera, with an acquisition time of 300 ms for the fluorescence images.

Experimental Setup for Spermatozoon/Oocyte Interaction Force Measurements. Our experimental setup is an adaptation of the biomembrane force probe[15] using a force transducer made of a biotinylated red blood cell maintained by a albumin-coated glass pipet and with a streptavidin-coated glass microbead attached to the

(27) Puech, P. H.; Poole, K.; Knebel, D.; Muller, D. J. *Ultramicroscopy* **2006**, *106*, 637−644.
(28) Afrin, R.; Yamada, T.; Ikai, A. *Ultramicroscopy* **2004**, *100*, 187−195.
(29) Benoit, M.; Gabriel, D.; Gerisch, G.; Gaub, H. E. *Nat. Cell Biol.* **2000**, *2*, 313−317.
(30) Zhang, X.; Chen, A.; De Leon, D.; Li, H.; Noiri, E.; Elitok, S.; Moy, V. T.; Goligorsky, M. S. *J. Am. Soc. Nephrol.* **2003**, *14*, 46A.
(31) Simon, A.; Durrieu, M. C. *Micron* **2006**, *37*, 1−13.
(32) Sun, M. Z.; Graham, J. S.; Hegedus, B.; Marga, F.; Zhang, Y.; Forgacs, G.; Grandbois, M. *Biophys. J.* **2005**, *89*, 4320−4329.
(33) Thoumine, O.; Ott, A.; Cardoso, O.; Meister, J. J. *J. Biochem. Biophys. Methods* **1999**, *39*, 47−62.
(34) Thoumine, O.; Ott, A. *Biorheology* **1997**, *34*, 309−326.
(35) Raucher, D.; Sheetz, M. P. *Biophys. J.* **1999**, *77*, 1992−2002.
(36) Li, Z. W.; Anvari, B.; Takashima, M.; Brecht, P.; Torres, J. H.; Brownell, W. E. *Biophys. J.* **2002**, *82*, 1386−1395.
(37) Cuvelier, D.; Chiaruttini, N.; Bassereau, P.; Nassoy, P. *Europhys. Lett.* **2005**, *71*, 1015−1021.
(38) Xu, G.; Shao, J. Y. *Biophys. J.* **2005**, *88*, 661−669.
(39) Evans, E.; Yeung, A. *Biophys. J.* **1989**, *56*, 151−160.
(40) Simon, S. I.; Nyunt, T.; Florine-Casteel, K.; Ritchie, K.; Ting-Beall, H. P.; Evans, E.; Needham, D. *Ann. Biomed. Eng.* **2007**, *35*, 595−604.
(41) Evans, E.; Heinrich, V.; Leung, A.; Kinoshita, K. *Biophys. J.* **2005**, *88*, 2288−2298.
(42) Heinrich, V.; Leung, A.; Evans, E. *Biophys. J.* **2005**, *88*, 2299−2308.
(43) Hosu, B. G.; Sun, M.; Marga, F.; Grandbois, M.; Forgacs, G. Eukaryotic membrane tethers revisited using magnetic tweezers. In 2007; p 67.
(44) Takahashi, Y.; Yamakawa, N.; Matsumoto, K.; Toyoda, Y.; Furukawa, K.; Sato, E. *Mol. Reprod. Dev.* **2000**, *56*, 412−423.
(45) Takahashi, Y.; Meno, C.; Sato, E.; Toyoda, Y. *Biol. Reprod.* **1995**, *53*, 424−430.
(46) Evans, J. P.; Foster, J. A.; McAvey, B. A.; Gerton, G. L.; Kopf, G. S.; Schultz, R. M. *Biol. Reprod.* **2000**, *62*, 76−84.

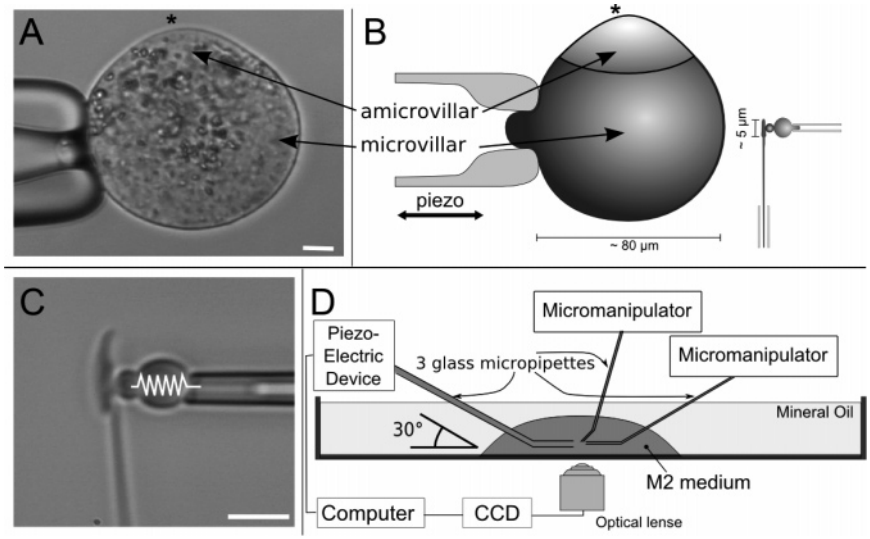

Figure 1. Experimental setup. (A) The oocyte is held by the left micropipette presenting the microvillar region to the probe. The amicrovillar region is indicated by the star. The scale bar is 10 μm. (B) Scheme of the three glass micropipettes showing a probe facing an oocyte and revealing the dimensions of the micropipettes as well as the size of the oocyte compared to the spermatozoon. (C) The probe is made of a red blood cell used as a spring, a streptavidin-coated bead attached to it via strong streptavidin−biotin bonds, and a spermatozoon adhering through nonspecific interactions to the bead. All of the elements are carefully aligned in the axis of the bent micropipette that holds the probe by the suction of the red blood cell. By controlling this suction, the stiffness k of the red blood cell is adjusted. The scale bar is 5 μm. (D) Schematic view of the whole experimental setup. The main drop of M2 medium is under mineral oil to prevent both evaporation at 37 °C and bacterial contamination. Real-time images acquired at 360 images/s by the CCD camera are used to compute the force of the interaction and control the piezo-electric device for precise positioning of the oocyte through online feedback control while the probe is fixed.

top through the formation of several streptavidin−biotin bonds. This traditional BFP probe is completed by the attachment of a cell to the bead, here a spermatozoon. The red blood cell is used as a spring with known stiffness that can be tuned by the aspiration pressure applied by the micropipette. The glass bead enables precise video tracking because when observed with a slightly unfocused optical microscope it displays a light spot with a Gaussian intensity profile at its center.[18]

For this experiment, three micropipettes with specific inner diameters were used. They were made from borosilicate glass capillary GC100-15 tubing (Harvard apparatus Ltd., Kent., U.K.) using a pipet puller (Sutter Instruments, model P-2000) and a homemade microforge. The micropipette holding the probe had an inner diameter of 1 to 2 μm, and the one used to manipulate the spermatozoon to assemble the probe and to maintain the flagellum throughout the experiment had a slightly larger inner diameter of 2−4 μm. The pipet holding the oocyte had an initial diameter of ∼40 μm and was then forged again to obtain a smaller inner diameter of 20 μm and to smooth rounded edges to prevent lysis during the manipulation of the oocyte. Each pipet was held in its own micromanipulator and connected to a combined hydraulic/pneumatic system that provided the necessary control of the aspiration force applied to the probe and cells. The micropipette holding the oocyte was coupled to a linear piezoelectric translator (Physik Instrumente, Karlsruhe, Germany) that allowed accurate control of the oocyte position. Using the microforge, all three pipettes were bent at a 30° angle in order to have the axisymmetric probe horizontal and aligned in the direction of the piezoelectric translator that moves the oocyte, as shown in Figure 1B.

The experiments were performed on the stage of a Leica inverted microscope (DMIRB type, Solms, Germany) positioned on an antivibration platform and equipped with a CCD camera (purchased form JAI, Yokohama, Japan), with a digitally controlled heating box (from Life Imaging Services GmbH, Reinach, Switzerland) maintaining the whole setup at 37 °C.

The experiments took place in a Petri dish filled with two 20 μL drops of M2 medium with 3% BSA under mineral oil (mouse embryo-tested light oil, density 0.84 g/mL, Sigma-Aldrich, Lyon, France). The first drop contained the sperm (at a sufficient concentration to maintain good viability of the cells), and the second one, some streptavidin-coated glass microbeads, the biotinylated red blood cells, and the oocytes. The first step of the experiment consisted of assembling the probe and began with the selection of a single hyperactive spermatozoon from the drop containing the sperm. A rapid stroke on its flagellum immobilized the spermatozoon. It was then aspirated into the pipet and transferred to the main drop. While maintaining the spermatozoon by its flagellum, the spermatozoon head was gently pushed into contact with a streptavidin-coated glass microbead for a few seconds. This forced contact resulted in robust bead/spermatozoon adhesion. This construct was then carefully manipulated into contact with a red blood cell held by a second albumin-coated micropipette in order to finalize the probe with maximum axisymmetric alignment (Figure 1C). During the force measurements, the flagellum of the spermatozoon was continuously held by the pipet at least 20 μm away from the head to keep the probe properly aligned, modifying the stiffness of the overall probe by less than 5%.

The force measurements consisted of performing a series of approach−contact−retraction cycles of the two gametes and measuring the interaction force felt by the gametes during the whole cycle. By translating the oocyte-holding pipet, the microvillar or amicrovillar area is brought in contact with the spermatozoon head and then pulled down (Figure 1A,B and 2). The speed and position of the oocyte were controlled over the approach and traction courses. The time of contact of the gametes and maximum compression forces at contact were also controlled. The interaction force experienced by the two gametes was continuously recorded by measuring the deformation of the red blood cell through a tracking procedure of the glass microbead at a rate of 360 frames/s. The interaction force $F(t)$ was equal to the red blood cell stiffness k multiplied by the elastic elongation of the red blood cell on the traction axis $\Delta l_t(t)$. The force is positive when the two cells are in compression and negative when in traction (Figure 2d). The interaction force is plotted as a function of the oocyte extension $\Delta l_o(t)$ in the traction axis, defined as the length difference of the oocyte in the traction axis at rest and under traction. When retracted at a constant speed v_{pull}, the extension of the oocyte $\Delta l_o(t)$ on the traction axis (Figure 3) is specified by the product of the retraction speed and time minus the deflection of the transducer $\Delta l_t(t)$ that is directly measured. If the origin of distance is taken when the force reaches zero during the pulling phase, then one can plot the interaction

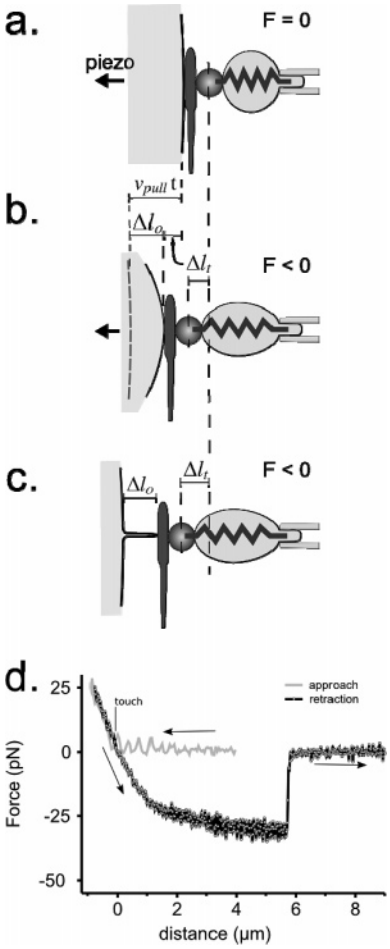

Figure 2. Schematics of the touch−retraction phase from the probe illustrating the springlike response of the probe and the oocyte response to traction at (a) touch ($F = 0$ pN), (b) during cell stretching, and (c) during tether elongation. (d) Approach−touch−retraction cycle force−distance curve. The force measured by the probe is expressed as a function of oocyte extension Δl_o. During the approach (gray line), the force is zero until the two cells are in contact. During the compression phase, the force is positive. When the predefined maximum force F_{max} is reached, the piezotranslator starts moving the oocyte-holding pipet in the other direction (black line with brighter dots), the force decreases, and we set the reference position to $\Delta l_o = 0$ when the force comes back to zero or changes sign during the retraction phase. The force becomes negative if an adhesion occurs and jumps back to zero when the two cells are separated. (b) Three distances Δl_o, $v_{pull}t$, and Δl_t are used to represent the relation $\Delta l_o = v_{pull}t - \Delta l_t$, where $v_{pull}t$ is the speed of the oocyte-holding pipet and Δl_t is the elongation of the red blood cell measured by the displacement, relative to the equilibrium position, of the glass bead attached to it.

force experienced by the two cells as a function of the elongation of the oocyte membrane on the traction axis ($\Delta l_o(t) = v_{pull}t - \Delta l_t(t)$).

To get good statistics and to explore the maximum surface of the oocyte, such an approach−contact−retraction cycle was repeated about 60 times for at least 3 different contact zones including both microvillar and amicrovillar areas of the membrane oocyte and for tens of gamete couples.

Results and Discussion

Spermatozoon/Oocyte Adhesion: Extrusion of Tethers from the Membrane Oocyte. The first experiment performed to characterize oocyte/spermatozoon adhesion consisted of introducing with a micropipette a spermatozoon in the vicinity of an oocyte and observing the two gametes with a microscope. After a short time (from a few seconds to 1 or 2 min), the spermatozoon head spontaneously made contact with the oocyte. After contact and in spite of the unceasing movement of the flagellum (which is able to induce the rotation of the oocyte), the spermatozoon head rarely detached spontaneously from the oocyte. To characterize the adhesion of the two gamete membranes further, the adherent spermatozoon and oocyte were then pulled with micropipettes in order to take them apart. When the oocyte and the spermatozoon were apparently separated and if the aspiration maintaining the oocyte on the pipet tip was stopped, the oocyte left the pipet in a direction toward the spermatozoon and reattached to it. This behavior reveals the formation of one or several tethers when the gametes are separated.

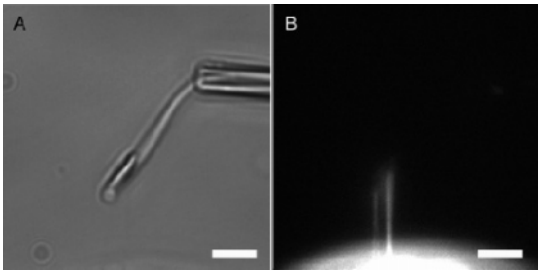

Figure 3. Tethers obtained after the separation of an oocyte labeled with anti-CD9 rat antibody coupled with goat anti-rat Alexa Fluor 594 in contact for 5 min with a normal spermatozoon in direct light microscopy (A) and under fluorescent excitation revealing only the tethers and the oocyte (B). The scale bar is 5 μm.

Most of the time, tethers are too thin to be observed with traditional light microscopy. To determine the origin of the tethers, fluorescence microscopy experiments were performed. It was necessary to use a fluorescent probe that remained at the oocyte surface and was distributed over the whole membrane. Because CD9 proteins were reported to be present in both microvillar and amicrovillar regions of the oocyte,[6] we chose anti-CD9 rat antibody as the fluorescent probe. Tethers that form between oocytes labeled with anti-CD9 rat antibody coupled with a goat anti-rat Alexa Fluor 594 and normal spermatozoon were fluorescent, whereas the spermatozoon did not become fluorescent (Figure 3B). This means that spermatozoon and oocyte membranes had not fused and therefore that tethers are exclusively composed of molecules from the oocyte membrane.

These experiments have provided qualitative information both on sperm/oocyte membrane adhesion and on the mechanical properties of the oocyte. The possibility of extruding tethers from the oocyte plasma membrane assumes that the molecular bonds involved in the adhesion of the gamete membranes are strong enough to resist the traction force applied to form the tethers. Tether formation has been observed in various systems,[32,35−38,40−42] but to our knowledge, this is the first evidence that some primary cells that interact in a physiological context during fertilization are able to form such tethers.

Force/Distance Measurements of Spermatozoon/Oocyte Interaction. To get more quantitative information, we have directly measured the forces involved in the adhesion of the spermatozoon head with the oocyte plasma membrane as well as those involved in the deformation of the oocyte membrane. Because of the morphological and functional differences between the microvillar and amicrovillar regions of the oocyte, both areas have been probed and compared. The experiment consists of bringing into contact the oocyte with the spermatozoon head and measuring the interaction force experienced by the cells during the whole separation phase. The number of bonds created during the contact of two objects varies with the concentration and distribution of the molecules or molecular complexes responsible for the adhesion. All of the quantitative cell force experiments

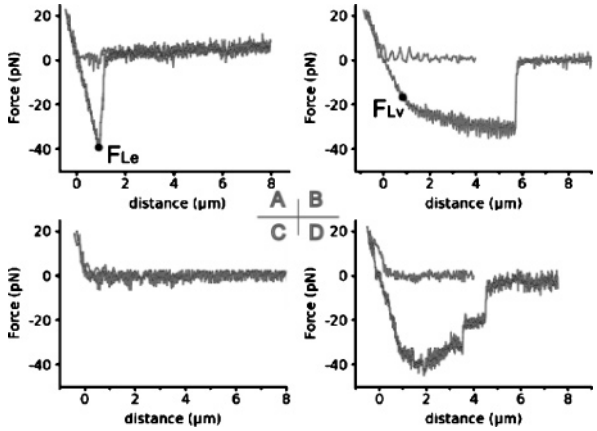

Figure 4. Typical force−distance curves of the approach−retraction cycles of the oocyte on the spermatozoon. During the approach phase, the force is zero until the cells are in contact, as revealed by a force increase of up to 20 pN. (A) Single attachment point with elastic behavior: upon traction, the oocyte is stretched, and the force increases linearly with distance, indicating an elastic response. When the cells are separated, the force jumps from a maximum force of F_{Le} to zero. (B) Single attachment point with elastic behavior and a damped regime: elastic deformation of the oocyte up to a force of F_{Lv}, followed by a transition to a damped regime, with extrusion of a tether from the oocyte membrane. (C) No attachment between the gamete membranes; upon traction, the interaction force decreases back to zero as the two cells are separated from each other. (D) Multiple attachment points: a complex force−distance curve with a succession of force jumps.

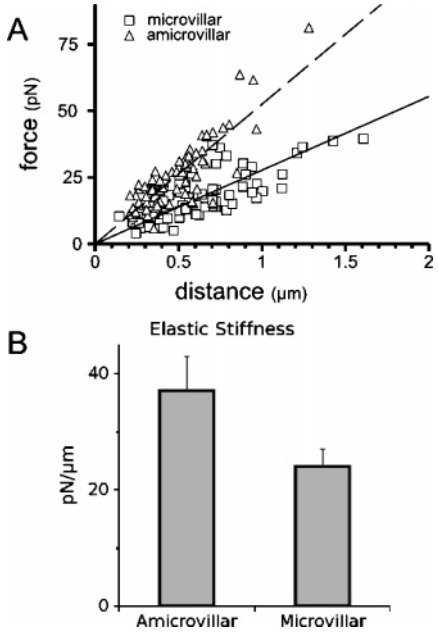

Figure 5. (A) Forces at the end of the elastic regime vs oocyte elongation for a single oocyte−spermatozoon couple recorded in the microvillar (□) and the amicrovillar (△) regions. The two regions show different elastic stiffnesses, and the corresponding force−distance curves are well fitted linearly (microvillar region, −; amicrovillar region, ---). (B) Mean (and standard error) stiffness for the amicrovillar and microvillar regions ($n = 15$ oocytes).

previously performed with AFM,[27−34] BFP,[16−18] or other dual pipet assay techniques[24,26,47] involved the use of functionalized surfaces, vesicles, or cell lines for which the molecular concentration and distribution parameters can be adjusted. In this study, we used primary cells that imply that the molecular concentration and distribution are imposed. A possible way of limiting the number of attachments in the spermatozoon/oocyte system is to optimize the area and time of contact by adjusting both the maximum compression force at contact and the approach speed of the cells. The contact time is the time for which cells are under compression. It starts with the two cells coming into contact, continues with the force of the interaction increasing up to a maximum compression force, and then ends with the force decreasing back to 0 pN. Satisfactory conditions were obtained for a red blood cell stiffness of 125 pN/μm, a 10 μm/s approach speed of the oocyte-holding pipet, and a maximum compression force of 20 pN without pause before the beginning of the retraction phase at 4 μm/s. Under these conditions, the total time spent by the cells under compression was around 250 ms. Indeed, under such experimental conditions, 15% of gamete contacts gave rise to well-defined single attachment (Figure 4A,B). For 60% of touches, no adhesions were detected (Figure 4C). The last 25% of touches gave rise to different kinds of interactions, including very complex profiles for which multiple attachment points are involved (Figure 4D). These proportions were identical (within 10%) for both microvillar and amicrovillar areas.

The part of the force−distance curve corresponding to the approach phase is always the same (i.e. force is zero until the cells come into contact) and then increases up to a value set by the operator (20 pN). When no attachment occurs (Figure 4C), the force decreases back to zero as the two cells are separated from each other. If an adhesion occurs, then the interaction force becomes negative during the traction phase before jumping back up to zero. The shapes of the force−distance curves in the separation phase vary considerably with the nature of the interaction. For instance, force−distance curves obtained from multiple attachment points are very complex, and even if the succession of jumps of forces observed in such cases (Figure 4D) may be attributed to the successive rupture of the attachment points, further interpretation is quite hazardous. In this study, we have focused on the 15% of touches giving single attachment events (Figure 4A,B). At the start of separation, the oocyte deformation always increases linearly with force, indicating an elastic response to the oocyte's stretching. Then two behaviors are observed: either the membranes completely separate (Figure 4A) or there is a transition to a damped regime (Figure 4B). This second regime corresponds to viscoelastic behavior of the oocyte plasma membrane associated with the extrusion of a tether. In the $F = f(\Delta l_o)$ representation given in Figure 4, the maximal elastic elongation experienced by the oocyte membrane and the local elastic stiffness of the oocyte membrane are directly accessible on the experimental curves. Indeed, the first one is given by the end distance of the elastic regime (x coordinate of F_{Le} in Figure 4A and F_{Lv} in Figure 4B). The local elastic stiffness of the membrane is the slope of the linear decrease in force with distance.

Stronger Membrane Elastic Stiffness in the Amicrovillar Area. A systematic study of the local elastic stiffness of the membrane has been performed both in the microvillar and amicrovillar areas of the oocyte. If, for one given couple of spermatozoon and oocyte, we plot the force at the end of the linear regime as a function of the associated membrane deformation (Δl_o), then the data can be well fitted linearly, with slopes corresponding to two distinct stiffness regimes. Data obtained for several positions inside the amicrovillar region are associated with the high-stiffness regime, and that obtained for the microvillar region, with the lower-stiffness regime (Figure 5A).

This means that the membrane stiffness values measured from distinct traction positions in each area are quite stable. From one

(47) Martinez-Rico, C.; Pincet, F.; Perez, E.; Thiery, J. P.; Shimizu, K.; Takai, Y.; Dufour, S. *J. Biol. Chem.* **2005**, *280*, 4753−4760.

oocyte to another, the stiffness values can change significantly (from 15 to 35 pN/μm for the microvillar region and from 22.5 to 60 pN/μm for the amicrovillar area), but for a given oocyte, the stiffness in the amicrovillar area is always on average 48% stronger than in the microvillar region. The dispersion of the stiffness values from one oocyte to another (37 $\pm$ 6 pN/μm for amicrovillar areas and 24 $\pm$ 3 pN/μm for microvillar regions, Figure 5B) may be attributed to different factors. The age of the oocytes could be invoked because experiments were performed with oocytes probed between 3 and 5 h after hyaluronidase and tyrode acid treatments. These chemical treatments performed during oocyte preparation could be responsible for the modification of the expression level of surface adhesion proteins. However, oocytes are reported to recover a good level of expression for a maximum fertilization rate after the 3 h recovery procedure.[44,45] The last factor for such a dispersion of the stiffness data is the natural inhomogeneities in a population of cells, inherent to biological material.

Even for a single attachment point between the gamete membranes, the elastic deformation of the oocyte membrane is perceptible on a surface of a few tens of square micrometers. The elastic stiffness that we measure therefore accounts for the elastic properties of the membrane on this scale. The fact that its value is consistent from one traction point to another inside the same area means that on the scale of a few tens of square micrometers the inhomogeneities in molecular composition of the membrane and in the interaction with the cytoskeleton are averaged. The significant differences in the stiffness values for amicrovillar and microvillar areas are probably correlated to the molecular composition of the membrane, which is different in the two regions.[5,6] The denser cytoskeleton network in the amicrovillar area,[46] responsible for the pear shape of the oocyte, is also likely to be involved in the stronger stiffness value measured in the amicrovillar area. Indeed, the cell membrane is connected to the cytoskeleton through molecular bonds.[48,49] Before the rupture of these bonds, a deformation of the membrane oocyte also involves the deformation of the cytoskeleton. A denser cytoskeleton network should therefore exhibit a stronger resistance to deformation. Such behavior is perfectly consistent with the higher stiffness measured in the amicrovillar area of the oocyte.

Elastic and Viscoelastic Response of the Membrane Oocyte to Mechanical Traction. Two types of force−distance curves are obtained with contacts producing single attachment events. Either the initial elastic regime is followed by the viscoelastic one in the same force−distance curve (Figure 4B) or the attachment point breaks directly during the elastic regime of the plasma membrane and no viscoelastic behavior is detected (Figure 4A). These two types of curves (A and B) were observed both in the microvillar and amicrovillar areas of the oocyte. Transition from an elastic to a viscoelastic regime has recently been reported by Evans and co-workers[41,42] on human neutrophils (PMN), whose membranes are rich in microvilli. According to these authors,[41] this transition from the elastic to the viscoelastic regime would be the signature of membrane detachment from the inner cytostructures. In this study, the tether formation rates are respectively 30% and 51% in the amicrovillar and microvillar regions. These results show than even if it is less probable, tethers can also be extruded from the amicrovillar region.

Figure 6 gives the histograms of F_{Le} and F_{Lv} forces corresponding to the end of the linear regime for both types (Types A and B of Figure 4) of curves under the experimental conditions

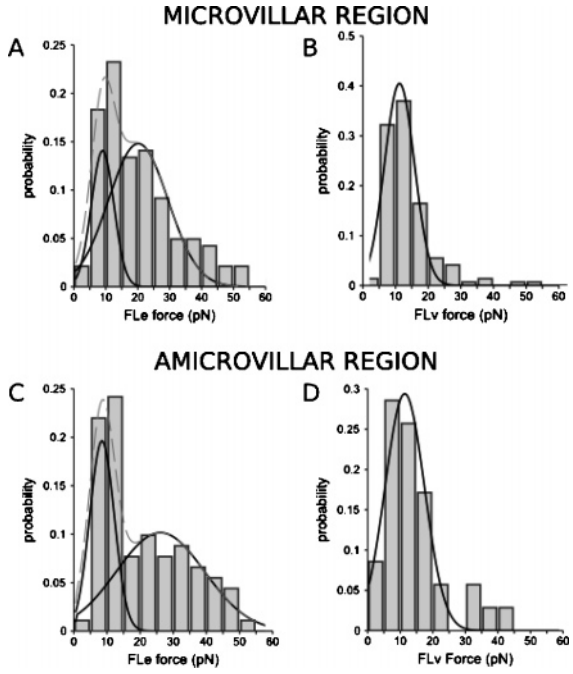

Figure 6. Histograms of force distributions for (A) F_{Le} and (B) F_{Lv} forces in the microvillar region and (C) F_{Le} and (D) F_{Lv} forces in the amicrovillar region. (A, C) Two peaks are shown. In each plot, the lower peak corresponds to bonds occurring in the v domain that break before any tether can be formed, and the high-force peak is related to rupture forces in the e domain.

described above with an effective loading rate of about 100 pN/s. Figure 6A,C corresponds to the F_{Le} forces obtained for curves without a viscoelastic regime in the amicrovillar and microvillar regions, respectively. Figure 6B,D gives the F_{Lv} forces resulting from the curves with two regimes, in the microvillar and amicrovillar regions. The shape of the histograms and the range of forces involved are similar in the microvillar and amicrovillar areas of the oocyte, but they significantly depend on the type of experimental curves. Indeed, the F_{Le} histograms show two distinct force distributions with the most probable forces centered around 8.5 and 19.5 pN for the microvillar area and around 8 and 25.5 pN for the amicrovillar area. By contrast, the F_{Lv} histogram shows a single peak centered around 11 pN in both the microvillar and amicrovillar areas. Because the second peak of the F_{Le} histogram corresponds to larger forces than in the F_{Lv} histogram, one can wonder why the oocyte membrane is able to remain elastic for traction forces much higher than typical forces at which a tether can be extruded. Apparently, exerting a high enough traction force on a strong enough attachment point somewhere on the oocyte is not a sufficient condition for creating a tether.

The location of the attachment point on the oocyte membrane appears to be a key parameter regarding the capability of the membrane to create a tether. This suggests that the oocyte membrane accessible to the spermatozoon is composed of different kinds of zones with different mechanical characteristics, some of them suitable for tether formation and the others not suitable. In the following text, the former zones will be referred to as v domains, and the latter, as e domains (Figure 7). When the attachment point between the spermatozoon and the oocyte membrane takes place on a v domain, the membrane is capable of undergoing a transition from the elastic to the viscoelastic regime. Even if speculative, the involvement of inhomogeneities of the spermatozoon in the possibility of binding to a v or e domain of the oocyte is probable. Indeed, the attachment points of the two gametes are most probably due to the recognition of

(48) Sun, Q. Y.; Schatten, H. *Reproduction* **2006**, *131*, 193−205.
(49) Sala-Valdes, M.; Ursa, A.; Charrin, S.; Rubinstein, E.; Hemler, M. E.; Sanchez-Madrid, F.; Yanez-Mo, M. *J. Biol. Chem.* **2006**, *281*, 19665−19675.

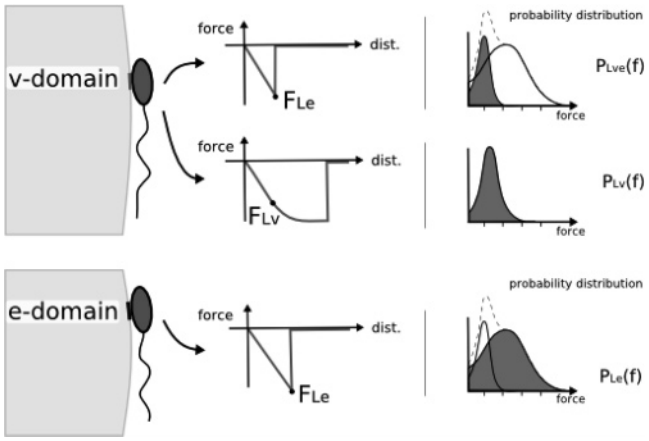

Figure 7. v and e domains on the oocyte membrane probed by the spermatozoon. From v domains, tethers can be extruded after the initial elastic deformation of the oocyte membrane. Two types of curves are therefore obtained depending on whether the elastic regime is followed by the viscoelastic one. From e domains, the membrane can deform only elastically. The curves obtained from v domains give rise to the F_{Lv} histogram and to the first peak of the F_{Le} histogram. The curves obtained from e domains give rise to the second peak of the F_{Le} histogram.

specific spermatozoon membrane ligands and molecular receptors present at the oocyte, and a bond is formed when they meet.

Because of the overlap of F_{Lv} and F_{Le} force distributions, the rupture of the membranes' attachment can also occur in v domains before any tether is formed and can therefore lead to purely elastic force behavior. In such a case, the experimental force−distance curve is similar to that obtained for membrane contacts occurring in an e domain (Figure 4A). Therefore, forces, which should have contributed to the F_{Lv} histogram if the attachment point between the gamete membranes had not broken, end up in the lower peak of the F_{Le} histogram (Figure 7). In other words, among the forces obtained at the end of the linear regime for gamete attachment in a v domain, a majority composes the F_{Lv} histogram, and the rest composes the first peak of the F_{Le} histogram. The second peak of the F_{Le} histogram comes from the spermatozoon/oocyte contacts situated in e domains of the oocyte.

It often happens that force−distance curves with only the elastic regime (type A in Figure 4) alternate with curves showing a tether extrusion (type B in Figure 4) during consecutive approach−retraction cycles. Let us take the example of the three consecutive approach−retraction cycles with the BAB sequence. According to the interpretation of the lower peak of the F_{Le} histogram (Figure 6), two cases have to be considered. In case 1, the attachment point always occurs in a v domain, which means that for the second cycle the link breaks before a tether starts to be extruded. In case 2, the attachment point occurs in a v domain during the first and third cycles and in an e domain during the second cycle. If the rupture force of the second cycle is within the range of forces typically observed in a v domain (<30 pN, Figure 6B,D), then it will not be possible to determine if the sequence corresponds to case 1 or 2. By contrast, if the rupture force of the second cycle is >30 pN, then only case 2 matches the sequence of events. In most of the series performed, the BAB sequence corresponding to case 2 was obtained and alternated with other sequences in the same contact area. This result proves that e and v domains can be present in a given contact area (10 μm^2). The fact that they can be discriminated suggests their small extension.

It is possible to predict the two peaks in Figure 6A,C in terms of probabilities. Let us define $P_{Lv}(f)\,df$ as the probability that a tether is extruded between f and $f + df$ and $P_{Le}(f)\,df$ as the probability that a rupture event happens between f and $f + df$. In such a description, the probability $P_{Lve}(f)\,df$ that a bond located in a v domain breaks at a traction force between f and $f + df$ in the initial elastic regime is the product of $P_{Le}(f)\,df$ and $(1 - \int_0^f P_{Lv}(f)\,df)$, which is the probability that under a traction force equal to f a tether has not yet begun to be elongated. It can therefore be expressed as

$$P_{Lve}(f)\,df = (1 - \int_0^f P_{Lv}(f)\,df)P_{Le}(f)\,df \qquad (1)$$

$P_{Lv}(f)$ is given by the F_{Lv} distribution, and $P_{Le}(f)$ will be approximated by the second peak of the F_{Le} distribution. $P_{Lve}(f)$ can be obtained by approximating $P_{Lv}(f)$ and $P_{Le}(f)$ by two Gaussian fits corresponding to the F_{Lv} peak and the second peak of F_{Le}, respectively (Figure 6A,C). From these fits, it is possible to predict the most probable force f^*_{Lve}. Independently, it is possible to adjust the F_{Le} histogram by two Gaussian distributions and obtain an experimental value for f^*_{Lve}. In Table 1, we reported the most probable forces f^*_{Lv}, f^*_{Le}, and f^*_{Lve} obtained from the Gaussian fits. The experimental f^*_{Lve} is also compared to the predicted one. Agreement is excellent both in the microvillar and amicrovillar regions. The experimental and predicted proportions of the one attachment point events occurring in a v domain that breaks in the elastic regime are also reported in Table 1.

Table 1. Most Probable Forces f^*_{Lv}, f^*_{Le}, and f^*_{Lve} in Both Microvillar and Amicrovillar Regions[a]

		microvillar	amicrovillar
f^*_{Lv} (pN)	exp	11	11
f^*_{Le} (pN)	exp	19.5	25.5
f^*_{Lve} (pN)	predicted	9	8.5
	exp	8.5	8
% of gamete attachment in a v domain broken in the elastic regime	predicted	20	14
	exp	18	47
% of gamete attachment	v domain	62	57
	e domain	38	43

[a] For f^*_{Lve}, both experimental and predicted most probable forces are given. Predicted and experimental percentages of attachment in v domains that ended before the transition with the viscoelastic regime. Percentage of attachment in e and v domains in both microvillar and amicrovillar regions.

The consistency between experimental and predicted data is very good in the microvillar area. The difference between the predicted and experimental data in the amicrovillar area may indicate that in this area a non-negligible number of curves just underwent the transition to the viscoelastic regime when the rupture event happened and were counted as elastic curves because of uncertainty while sorting the curves. An alternate explanation could be that approximating $P_{Le}(f)$ by the second peak of the F_{Le} distribution is not a valid assumption in the amicrovillar region. This would indicate that molecular bonds involved in the amicrovillar e and v domains are different.

From the experimental evaluation of the rate of gamete attachment in a v domain that breaks in the elastic regime, it is possible to give the proportions of the one attachment point occurring in the e and v domains (Table 1). v and e domains are both distributed over the entire oocyte surface, and they are almost equally accessible in amicrovillar and microvillar areas.

f^*_{Le} is the only experimental data that provides information on the robustness of the link between the gamete membranes. One

can note that f^*_{Le} is higher in the amicrovillar area than in the microvillar region. This result tends to show that in e zones the type of links involved in the spermatozoon/oocyte adhesion are different in the microvillar and microvillar areas. This indicates that proteins and/or molecular arrangement involved in the spermatozoon/oocyte adhesion are different in both areas.

Conclusions

This experimental study deals with the interaction between an oocyte and a spermatozoon and with the mechanical properties of the oocyte membrane. The first approach combining micropipette manipulation and fluorescence microscopy has shown that when a spermatozoon is in contact with the oocyte plasma membrane it rarely detaches spontaneously in spite of the large movements of its flagellum. When separation is forced after a long contact time, tethers connecting the cells are extruded from the oocyte membrane. With a BFP adapted to cell−cell measurements, we have measured the interaction forces experienced by the two gametes when they are brought into contact and then pulled apart from each other. Microvillar and amicrovillar areas of the oocyte surface have been systematically probed and compared. We found that the amicrovillar area is characterized by an average elastic stiffness that is substantially stronger (48%) than the amicrovillar area, which is consistent with a denser cytoskeleton network in this area.[46] The experiments have revealed the presence of two types of membrane domains of micrometer sizes or smaller, distributed or at least accessible in comparable proportions in both microvillar and amicrovillar areas. The mechanical properties of these domains are different. In an e domain, the membrane deforms only elastically under traction, whereas in a v domain the elastic regime can be followed by a viscoelastic one. In the latter case, tethers can be extruded from the oocyte membrane. As a result, tethers can be extruded in microvillar regions in agreement with what was observed with other types of microvillar membranes[41,42] but also in amicrovillar areas. In spite of an equal distribution of e and v domains over the entire oocyte surface, tethers are more often observed in the microvillar area. A possible explanation is that the molecules involved in the spermatozoon−oocyte link in a v domain are different in the microvillar and amicrovillar areas. In such a case, the binding would be stronger in the amicrovillar region. Another explanation may be the stronger binding of the membrane to the cytoskeleton in the amicrovillar area. In the e domains, spermatozoon/oocyte links are significantly stronger in the amicrovillar than in the microvillar area. This tends to show that proteins and/or molecular arrangement involved in the spermatozoon/oocyte adhesion are different in microvillar and amicrovillar areas. Because the attachment points of the two gametes are most probably due to the recognition of specific spermatozoon membrane ligands and molecular receptors present at the oocyte surface, both oocyte and spermatozoon molecular arrangements play a decisive role. To create a bond, such receptors and associated ligands have to meet. The rate of bond formation will therefore depend on the molecular inhomogeneities of both oocyte and spermatozoon membranes.

This study has therefore proved the capability of the modified BFP technique used here in quantitatively measuring local changes in gamete membrane adhesion and in probing the mechanical behavior of the oocyte membrane on the micrometer scale. The nature of the e and v domains and the molecular players involved in the microvillar and amicrovillar areas of the oocyte and at the spermatozoon membrane remain to be further investigated. This can be achieved by combining the approach presented here and strategic antibody molecules, knock-out gametes, or drugs modifying the binding between the cell membrane and its cytoskeleton. This approach could therefore become an efficient way of studying the molecular basis of spermatozoon/oocyte plasma membrane interaction during mammalian fertilization, which is very complementary to the usual biological strategies.[5,50,51] With the latter, it is often impossible to discriminate whether the involved proteins play a role in adhesion, fusion, or both steps of fertilization. By contrast, here, gamete adhesion is probed independently from fusion. Moreover, it allows the study of gamete adhesion under conditions close to physiological ones because two isolated gametes are involved the same way as in fertilization.

LA702258X

(50) Evans, J. P. *Hum. Reprod. Update* **2002**, *8*, 297−311.
(51) Kaji, K.; Kudo, A. *Reproduction* **2004**, *127*, 423−429.